This article was downloaded by:
On: *14 January 2011*
Access details: *Access Details: Free Access*
Publisher *Taylor & Francis*
Informa Ltd Registered in England and Wales Registered Number: 1072954 Registered office: Mortimer House, 37-41 Mortimer Street, London W1T 3JH, UK

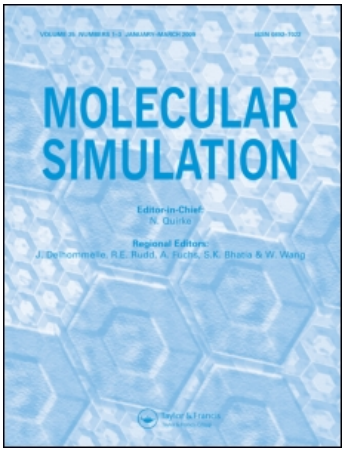

Molecular Simulation
Publication details, including instructions for authors and subscription information:
http://www.informaworld.com/smpp/title~content=t713644482

Modulated Self-Organization in Complex Amphiphilic Systems

J. G. E. M. Fraaije[a]; A. V. Zvelindovsky[a]; G. J. A. Sevink[a]; N. M. Maurits[a]
[a] University of Groningen, AG Groningen, The Netherlands

To cite this Article Fraaije, J. G. E. M. , Zvelindovsky, A. V. , Sevink, G. J. A. and Maurits, N. M.(2000) 'Modulated Self-Organization in Complex Amphiphilic Systems', Molecular Simulation, 25: 3, 131 — 144
To link to this Article: DOI: 10.1080/08927020008044119
URL: http://dx.doi.org/10.1080/08927020008044119

PLEASE SCROLL DOWN FOR ARTICLE

Full terms and conditions of use: http://www.informaworld.com/terms-and-conditions-of-access.pdf

This article may be used for research, teaching and private study purposes. Any substantial or systematic reproduction, re-distribution, re-selling, loan or sub-licensing, systematic supply or distribution in any form to anyone is expressly forbidden.

The publisher does not give any warranty express or implied or make any representation that the contents will be complete or accurate or up to date. The accuracy of any instructions, formulae and drug doses should be independently verified with primary sources. The publisher shall not be liable for any loss, actions, claims, proceedings, demand or costs or damages whatsoever or howsoever caused arising directly or indirectly in connection with or arising out of the use of this material.

Molecular Simulation, 2000, Vol. 25, pp. 131–144
Reprints available directly from the publisher
Photocopying permitted by license only

© 2000 OPA (Overseas Publishers Association) N.V.
Published by license under
the Gordon and Breach Science
Publishers imprint.
Printed in Malaysia.

MODULATED SELF-ORGANIZATION IN COMPLEX AMPHIPHILIC SYSTEMS

J. G. E. M. FRAAIJE*, A. V. ZVELINDOVSKY,
G. J. A. SEVINK and N. M. MAURITS

University of Groningen, Nijenborgh 4, 9747 AG Groningen, The Netherlands

(Received April 1999; accepted May 1999)

Downloaded At: 18:55 14 January 2011

We discuss novel simulation methods for 3D pattern formation in complex amphiphilic systems. The focus is on the supra-molecular or mesoscopic level. The building blocks consist of sequences of dissimilar monomers, connected in copolymer chain molecules. Internal factors such as composition and architecture of the polymers, but also external factors such as applied shear, embedded reactions and level of confinement control the self-organization phenomena. Specific examples include dynamical pattern formation in polymer surfactant solution, reactive polymer blends and surface directed structure formation in block copolymer liquids. The approach lives in a twilight zone between scientific disciplines. The ambitious goal is the invention of methods for the rational design of truly complex bio-mimicking materials, in which we combine principles from chemical engineering, physics, chemistry and biology. The keyword is self-organization, of course. But do not be mistaken: autonomous self-organization leads to trouble, modulated self-organization leads to beauty.

Keywords: Block copolymer; morphology; shear; surface; reaction

INTRODUCTION

For a long time, chemical engineers have analyzed macroscale properties using a variety of continuum mechanics models. In the last decade molecular modeling has grown to an essential part of research and development in the chemical and pharmaceutical industries. Despite the considerable success of both molecular and macroscale modeling, in the past few years it has become more and more apparent that in many materials mesoscale structures determine material properties to a very large extent. Mesoscale

*Corresponding author.

structures are typically of the size of 10 to 1000 nm. The industrial relevance of mesoscale modeling is obvious, nevertheless the necessary general purpose computational engineering tools are absent.

We are developing a general purpose method for mesoscale soft-condensed matter computer simulations, based on a functional Langevin approach for mesoscopic phase separation dynamics of complex polymer liquids. This project aims to consider topics of utmost importance in chemical engineering, such as chemical reactions, convection and flow effects, surfaces and boundaries, *etc.*

The morphology formation in complex liquids has been studied by many authors using time dependent Landau-Ginzburg models [1–5]. These models are based on traditional free energy expansion methods (Cahn–Hilliard [6], Oono–Puri [7], Flory-Huggins-de Gennes [8]) which contain only the basic physics of phase separation [9] and are not well suited for specific application to the different complex industrial and biological liquids. In contrast to these phenomenological theories we use dynamic density functional theory [9–15] where we do not truncate the free energy at a certain level, but rather retain the full polymer path integral by a numerical procedure. Very recently Kawakatsu and Doi started to use a similar approach [16, 17].

Downloaded At: 18:55 14 January 2011

Although calculation of polymer path integrals is computationally very intensive, it allows us to describe mesoscopic dynamics of a specific complex polymer liquid [18].

The prediction of the mesoscale morphology of complex polymer systems is very important for the final product properties. The application area of the proposed method includes computer simulation of such processes as emulsion copolymerization, copolymer melts and softened polymer melts, polymer blends, polymer surfactant stabilized emulsions, and adsorption phenomena in aqueous surfactant systems.

In this paper we demonstrate only several types of modulation of self-assembly in complex polymer systems. They are: shearing of concentrated aqueous solution of amphiphilic polymer surfactant, shearing of symmetric diblock copolymer blend, reactions in polymer mixture, surface directed phase separation in copolymer melt.

DYNAMIC DENSITY FUNCTIONAL THEORY

We give a short outline of the theory of the mesoscopic dynamics algorithms. For more details see Ref. [11]. We consider a system of n Gaussian chains of N beads of several different species (for example, $A_{N_A}B_{N_B}$,

$N = N_A + N_B$ for diblock copolymer, $E_{N_E}P_{N_P}E_{N_E}, N = N_P + 2N_E$ for symmetric triblock copolymer). The solvent can be easily taken into account [18]. The volume of the system is V. There are concentration fields $\rho_I(\mathbf{r})$, external potentials $U_I(\mathbf{r})$ and intrinsic chemical potentials $\mu_I(\mathbf{r})$.

Imagine that on a course-grained time scale, there is a certain collective concentration field $\rho_I(\mathbf{r})$ of the beads of type I(say, A or B). Given this concentration field a free energy functional $F[\rho]$ can be defined as follows:

$$\beta F[\rho] = -n \ln \Phi + \ln n! - \beta \sum_I \int U_I(\mathbf{r}) \rho_I(\mathbf{r}) d\mathbf{r} + \beta F^{\text{nid}}[\rho] \tag{1}$$

Here Φ is the partition functional for the ideal Gaussian chains in the external field U_I, and $F^{\text{nid}}[\rho]$ is the contribution from the non-ideal interactions. The free energy functional (1) is derived from an optimization criterium (see [11]) which introduces the external potential as a Lagrange multiplier field. The external potentials and the concentration fields are related *via* a density functional for ideal Gaussian chains:

$$\rho_I[U](\mathbf{r}) = n \sum_{s'=1}^{N} \delta_{Is'}^K \text{Tr}_c \psi \delta(\mathbf{r} - \mathbf{R}_{s'}) \tag{2}$$

Here $\delta_{Is'}^K$ is a Kronecker delta function with value 1 if bead s' is of type I and 0 otherwise. The trace Tr_c is limited to the integration over the coordinates of one chain

$$\text{Tr}_c(\cdot) = \mathcal{N} \int_{V^N} (\cdot) \prod_{s=1}^{N} d\mathbf{R}_s$$

$\mathcal{N}$ is a normalization constant. ψ is the single chain configuration distribution function

$$\psi = \frac{1}{\Phi} e^{-\beta \left[H^G + \sum_{s=1}^{N} U_s(\mathbf{R}_s) \right]} \tag{3}$$

where H^G is the Gaussian chain Hamiltonian

$$\beta H^G = \frac{3}{2a^2} \sum_{s=2}^{N} (\mathbf{R}_s - \mathbf{R}_{s-1})^2 \tag{4}$$

with a the Gaussian bond length parameter. The density functional is bijective; for every set of fields $\{U_I\}$ there is exactly one set of fields $\{\rho_I\}$. Thus there exists a *unique* inverse density functional $U_I[\rho]$. There is no

Downloaded At: 18:55 14 January 2011

known closed analytical expression for the inverse density functional, but for our purpose it is sufficient that the inverse functional can be calculated efficiently by numerical procedures.

We split the non-ideal free energy functional formally into two parts

$$F^{\text{nid}}[\rho] = F^{c}[\rho] + F^{e}[\rho]$$

where F^{e} contains the excluded volume interactions, and F^{c} the cohesive interactions. The intrinsic chemical potentials μ_I are defined by the functional derivatives of the free energy:

$$\mu_I(\mathbf{r}) \equiv \frac{\delta F}{\delta \rho_I(\mathbf{r})} = -U_I(\mathbf{r}) + \frac{\delta F^{c}}{\delta \rho_I(\mathbf{r})} + \frac{\delta F^{e}}{\delta \rho_I(\mathbf{r})} \tag{5}$$

$$= -U_I(\mathbf{r}) + \mu_I^{c}(\mathbf{r}) + \mu_I^{e}(\mathbf{r}) \tag{6}$$

Here we have introduced the cohesive potential $\mu_I^{c}(\mathbf{r})$ and the excluded volume potential μ_I^{e}. For the cohesive interactions we employ a two-body mean field potential

$$F^{c}[\rho] = \frac{1}{2}\sum_{IJ}\iint \varepsilon_{IJ}(|\mathbf{r}-\mathbf{r}'|)\rho_I(\mathbf{r})\rho_J(\mathbf{r}')d\mathbf{r}d\mathbf{r}' \tag{7}$$

$$\mu_I^{c}(\mathbf{r}) \equiv \frac{\delta F^{c}}{\delta \rho_I} = \sum_{J}\int_{V} \varepsilon_{IJ}(|\mathbf{r}-\mathbf{r}'|)\rho_J(\mathbf{r}')d\mathbf{r}' \tag{8}$$

where $\varepsilon_{IJ}(|\mathbf{r}-\mathbf{r}'|) = \varepsilon_{JI}(|\mathbf{r}-\mathbf{r}'|)$ is a cohesive interaction between beads of type I at $\mathbf{r}$ and J at $\mathbf{r}'$ defined by the Gaussian kernel

$$\varepsilon_{IJ}(|\mathbf{r}-\mathbf{r}'|) \equiv \varepsilon_{IJ}^{0}\left(\frac{3}{2\pi a^2}\right)^{(3/2)} \mathrm{e}^{-(3/2a^2)(\mathbf{r}-\mathbf{r}')^2} \tag{9}$$

The excluded volume interactions can be included *via* the correction factor or insertion probability for each bead, c (see [12]):

$$\beta F^{e}[\rho] = -\sum_{I}\int_{V} \rho_I(\mathbf{r}) \ln c(\mathbf{r})d\mathbf{r} \tag{10}$$

The insertion probability is interpreted as the effective fraction of free space. The lower the fraction of free space, the lower the insertion probability and the higher the excess free energy. We have studied several models (van der Waals, Flory-Orwoll-Vrij, Carnahan-Starling) for the excess free energy function. We found that the phenomenological Helfald

Downloaded At: 18:55 14 January 2011

penalty function provides a numerically and mathematically simple way to account for compressibility effects in the system [12]. In equilibrium $\mu_I(\mathbf{r})$ is constant; this yields the familiar self-consistent field equations for Gaussian chains, given a proper choice for F^{nid}. When the system is not in equilibrium the gradient of the intrinsic chemical potential $-\nabla\mu_I$ acts as a thermodynamic force which drives collective relaxation processes. When the Onsager coefficients are constant the stochastic diffusion equations are of the following form

$$\frac{\partial \rho_I}{\partial t} = -\nabla \cdot \mathbf{J}_I \tag{11}$$

$$\mathbf{J}_I = -M\nabla\mu_I + \tilde{\mathbf{J}}_I \tag{12}$$

where M is a mobility coefficient and $\tilde{\mathbf{J}}_I$ is a noise field, distributed according to a fluctuation-dissipation theorem.

The further development of the theory includes hydrodynamic effects such as convection and the effect of shear on morphology formation [19].

Downloaded At: 18:55 14 January 2011

APPLICATION

Modulation by Shear

It is known that flow fields affect mesoscale structures in complex liquids and polymer systems, giving rise to global orientation [21,22]. Because of its industrial importance the behaviour of complex polymer liquids under shear is an intensively studied topic both experimentally and theoretically [23–25,28]. Most of the work is dedicated to the stability analysis of patterns and to phase transitions in complex polymer liquids under shear.

The time evolution of morphologies in complex liquids under shear was also studied in computer simulations using Landau type free energies in 2D geometries such as a square cell [3–5,21], a rectangle [1,2] and in a two-dimensional Couette flow [1]. Recently the shear effect in a 2D polymer system was studied using the path integral formalism for the kinetic coefficient [16]. However this was carried out for a model with simple periodic boundary conditions and a conventional phenomenological free energy.

The time evolution of the density field $\rho_I(\mathbf{r})$ under simple shear flow, $v_x = \dot{\gamma}y$, $v_y = v_z = 0$, can be described by dynamic equation (11) with a convective term

$$\dot{\rho}_I = M_I\nabla \cdot \rho_I\nabla\mu_I - \dot{\gamma}y\nabla_x\rho_I + \eta_I$$

where $\dot{\gamma}$ is the shear rate (the time derivative of the strain γ). For a $L \times L \times L$ cubic grid we use a sheared periodic boundary condition [26, 27]:

$$\rho(x, y, z, t) = \rho(x + iL + \gamma jL, y + jL, z + kL, t).$$

Figure 1 illustrates the application of our method for a 3D melt of block copolymers A_8B_8 under simple steady shear flow. Applying shear speeds up the lamellar formation in a diblock copolymer melt enormously. The alignment qualitatively differs from the 2D case – so called "perpendicular" lamellae are formed in 3D. From experiments and stability analysis this orientation is well known to be the most stable one (see *e.g.* [28]). The structure remains stable after switching off the shear.

Figure 2 demonstrates formation of hexagonal cylindrical phase in aqueous solution of triblock copolymer Pluronic L64, modelled as $E_3P_9E_3$.

Modulation by Reactions

In dynamic mean-field density functional theory, the dynamics of the polymer melt under simple steady shear is described by the time evolution

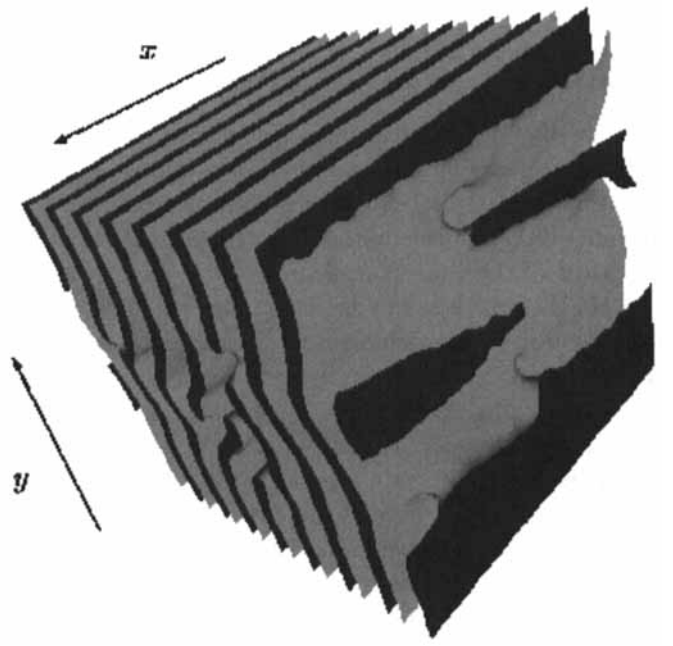

FIGURE 1 Isosurface representation of the A_8B_8 melt at $\tau = 75000$ and shear flow $v_x = \dot{\gamma}y$, $v_y = v_z = 0$, using the structure at $\tau = 500$ (Fig. 6) as a starting structure. The isolevel is $\theta_A = \nu\rho_A = 0.3$. One can clearly observe the global lamellar orientation. The x and y-axes are indicated.

Downloaded At: 18:55 14 January 2011

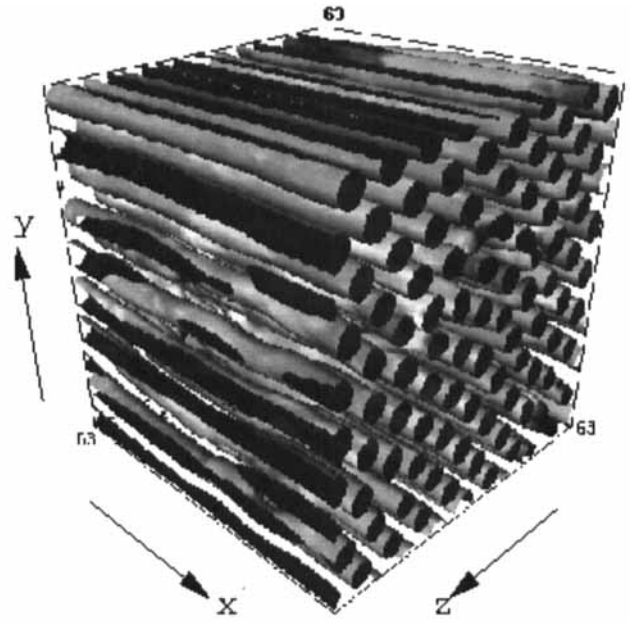

FIGURE 2 Mesophases of 55% Pluronic L64 in water under shear at time $\tau = 12500$. The isosurfaces are at $\theta_P \equiv \nu_P \rho_P = 0.33$. The x-axis is velocity direction, y-axis is velocity gradient direction and z-axis is neutral one.

Downloaded At: 18:55 14 January 2011

of density fields ρ_I. The dynamics is governed by a diffusion-convection equation with sheared periodic boundary conditions and can readily be extended with (second order) reaction terms in the following manner:

$$\frac{\partial \rho_I}{\partial t} = M\nabla \cdot \rho_I \nabla \frac{\delta F}{\delta \rho_I} - \dot{\gamma} y \nabla_x \rho_I + \sum_{J=1,K=1}^{N} k_{JK} \rho_J \rho_K + \eta_I. \tag{13}$$

Here M is a mobility parameter, $\dot{\gamma}$ is the shear rate, which is zero if no shear is applied, η_I is a stochastic term which is distributed according to a fluctuation-dissipation theorem [14] and k_{JK} is the reaction rate which can be either negative for reactants or positive for products. Notice that the reactive noise can be neglected here. Different order reactions or multiple reaction terms can be added without any difficulties, but as a proof of principle we focus here on the above type of reactions. In this subsection we study the effect of combined microphase separation, shear AND reaction to gain insight in the mechanisms that are important in pathway controlled morphology formation and in particular in reactive blending.

We therefore study a reaction in which a homopolymer A_8 couples to a homopolymer B_8 to form a diblock copolymer A_8B_8. The reaction is

limited to the endgroups and we assume that if two blocks that can couple are close enough, the reaction takes place. This reaction can be modeled as follows:

$$\begin{aligned}
\frac{\partial \rho_{hA}}{\partial t} &= M\nabla \cdot \rho_{hA}\nabla \frac{\delta F}{\delta \rho_{hA}} - \dot{\gamma} y \nabla_x \rho_{hA} - k\rho_{hA}\rho_{hB} + \eta_{hA} \\
\frac{\partial \rho_{hB}}{\partial t} &= M\nabla \cdot \rho_{hB}\nabla \frac{\delta F}{\delta \rho_{hB}} - \dot{\gamma} y \nabla_x \rho_{hB} - k\rho_{hA}\rho_{hB} + \eta_{hB} \\
\frac{\partial \rho_{dA}}{\partial t} &= M\nabla \cdot \rho_{dA}\nabla \frac{\delta F}{\delta \rho_{dA}} - \dot{\gamma} y \nabla_x \rho_{dA} + k\rho_{hA}\rho_{hB} + \eta_{dA} \\
\frac{\partial \rho_{dB}}{\partial t} &= M\nabla \cdot \rho_{dB}\nabla \frac{\delta F}{\delta \rho_{dB}} - \dot{\gamma} y \nabla_x \rho_{dB} + k\rho_{hA}\rho_{hB} + \eta_{dB}
\end{aligned} \tag{14}$$

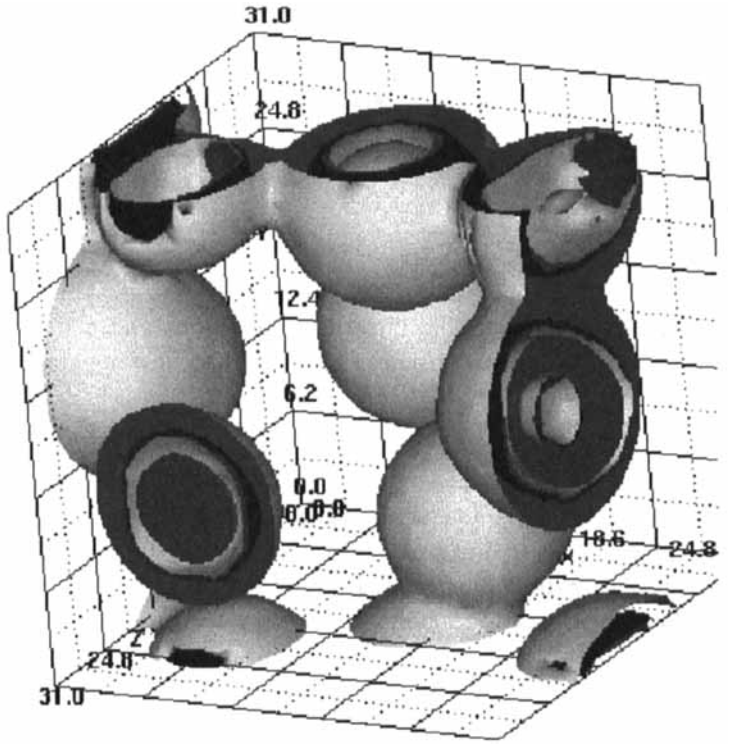

FIGURE 3 Three dimensional simulation of a homopolymer blend 90%/10% A_8/B_8. Before the reactions were switched on, 28000 steps of shear were performed ($\Delta\tau\dot{\gamma} = 0.001$) on the blend. The shear was stopped at $\tau = 28000$ and 2500 reaction steps were performed ($\Delta\tau k = 0.1$). In the figure the isodensity surfaces at different levels are depicted at $\tau = 30500$ of ρ_{hB} (yellow), ρ_{dA}(red) and ρ_{dB} (blue). The total volume fractions at this time level are 80.5% A_8, 0.5% B_8 and 19% A_8B_8.

Downloaded At: 18:55 14 January 2011

Here, ρ_{hA}/ρ_{hB} is the density of A/B beads in the homopolymer, ρ_{dA}/ρ_{dB} is the density of A/B beads in the diblock copolymer and k is the reaction rate of the coupling reaction.

Figure 3 gives an example of formation of double layer droplets in sheared reactive polymer system. Initially A/B blend was subject to shear which resulted in formation of elongated droplets. Then reaction on the surface of droplets took place after switching off shear. That leads to relaxation of elongation shape of droplets towards spherical one. Excess of polymer formed at interface goes inside the droplets which forms double layer structure.

Modulation by Geometry Constraints

The polymer melt is modeled as a compressible system, consisting of Gaussian chain molecules in a mean field environment. The free energy functional for copolymer melts has a form that is similar to the free energy that is used before:

$$\begin{aligned} F[\{\rho\}] = -kT \ln \frac{\Phi^n}{n!} - \sum_I \int_V U_I(\mathbf{r})\rho_I(\mathbf{r})d\mathbf{r} \\ + \frac{1}{2}\sum_{I,J} \int_{V^2} \varepsilon_{IJ}(\mathbf{r}-\mathbf{r}')\rho_I(\mathbf{r})\rho_J(\mathbf{r}')d\mathbf{r}d\mathbf{r}' \\ + \frac{1}{2}\sum_{I} \int_{V^2} \varepsilon_{IM}(\mathbf{r}-\mathbf{r}')\rho_I(\mathbf{r})\rho_M(\mathbf{r}')d\mathbf{r}d\mathbf{r}' \\ + \frac{\kappa_{IJ}}{2} \int_V \left(\sum_I \nu_I(\rho_I(\mathbf{r}) - \rho_I^0) \right)^2 d\mathbf{r} , \end{aligned} \tag{15}$$

except for an extra fourth term that contributes only in the direct vicinity of the filler particles. This accounts for the interaction of a polymer melt with surfaces. In this equation, n is the number of polymer molecules, Φ is the intra-molecular partition function for ideal Gaussian chains in an external field U, I is a component index, ρ_I are the density fields of the different bead types I and V is the system volume. Inside the filler particles, the densities ρ_I of the different bead types are equal to zero. Since the density ρ is present in all integrals in the definition of the free energy (15), integrals over the entire volume V are equal to the integrals restricted to V/V^0, standing for the total volume V with exception of the volume taken by the filler particles, denoted as V^0. The filler particles considered here are

Downloaded At: 18:55 14 January 2011

constrained to the condition of stationary position in time. The constant density field $\rho_M(M$ represents beads of the filler particle type) that appears in Eq. (15) is defined as $\rho_M(\mathbf{r})=1$ for $\mathbf{r}\in V^0$ and $\rho_M(\mathbf{r})=0$ for $\mathbf{r}\in V/V^0$. The average concentration ρ_I^0 is and ν_I is the particle volume. The surface interactions have kernels ε_{IM}. The Helfand compressibility parameter is κ_{IJ} [12].

The ensemble average particle density $\rho_s(\mathbf{r})$ of a certain bead s at position $\mathbf{r}$ in space is

$$\rho_s[U](\mathbf{r}) = C\mathcal{M}(\mathbf{r}) \int_{V^N} \psi(\mathbf{R}_1, \ldots, \mathbf{R}_N)\delta(\mathbf{r} - \mathbf{R}_s)d\mathbf{R}_1 \cdots d\mathbf{R}_N, \tag{16}$$

where C is a normalization constant and a mask field $\mathcal{M}(\mathbf{r})$ is used that is defined as

$$\mathcal{M}(\mathbf{r}) = \begin{cases} 0 & \mathbf{r}\in V^0 \\ 1 & \mathbf{r}\in V/V^0 \end{cases}$$

The density functional can be calculated *via* Green propagators (see [15] for details)

$$\rho_s(\mathbf{r}) \propto G_s(\mathbf{r})\sigma[G_{s+1}^{\text{inv}}](\mathbf{r}) \tag{17}$$

The set of once integrated Greens functions $G_s(r)$ and $G_{s+1}^{\text{inv}}(r)$ are related by the recurrence relations

$$\begin{aligned} G_s(\mathbf{r}) &= \mathcal{M}(\mathbf{r})\mathrm{e}^{-U_s(\mathbf{r})}\sigma[G_{s-1}](\mathbf{r}) \\ G_s^{\text{inv}}(\mathbf{r}) &= \mathcal{M}(\mathbf{r})\mathrm{e}^{-U_s(\mathbf{r})}\sigma[G_{s+1}^{\text{inv}}](\mathbf{r}) \end{aligned} \tag{18}$$

with $G_0(\mathbf{r}) = G_{N+1}^{\text{inv}}(\mathbf{r}) = 1$. The linkage operator $\sigma=\sigma[f](\mathbf{r})$ is defined as a convolution with a Gaussian kernel

$$\sigma[f](\mathbf{r}) = \left(\frac{3}{2\pi a^2}\right)^{(3/2)} \int_V \mathrm{e}^{-(3/2a^2)(\mathbf{r}-\mathbf{r}')^2} f(\mathbf{r}')d\mathbf{r}' \tag{19}$$

The time evolution of the density field $\rho_I(\mathbf{r})$ can be described by a time dependent Landau-Ginzburg type equations (11, 12). The boundary conditions that are used on the simulation box are periodic boundary conditions. For the diffusion flux in the vicinity of the filler particles, rigid-wall boundary conditions are used. A simple way to implement these boundary

Downloaded At: 18:55 14 January 2011

conditions in accordance with the conservation law is to allow no flux through the filler particle surfaces, *i.e.*,

$$\nabla \mu_I \cdot \mathbf{n} = 0, \tag{20}$$

where $\mathbf{n}$ is the normal pointing towards the filler particle. The same boundary conditions apply to the noise η_I. Figure 4 demonstrates formation of lamellar structure in A_8B_8 melt in presence of interacting walls.

In Figure 5 one can see the same system but confined between neutral walls. This confinements leads system to form "perpendicular" lamellae to the walls.

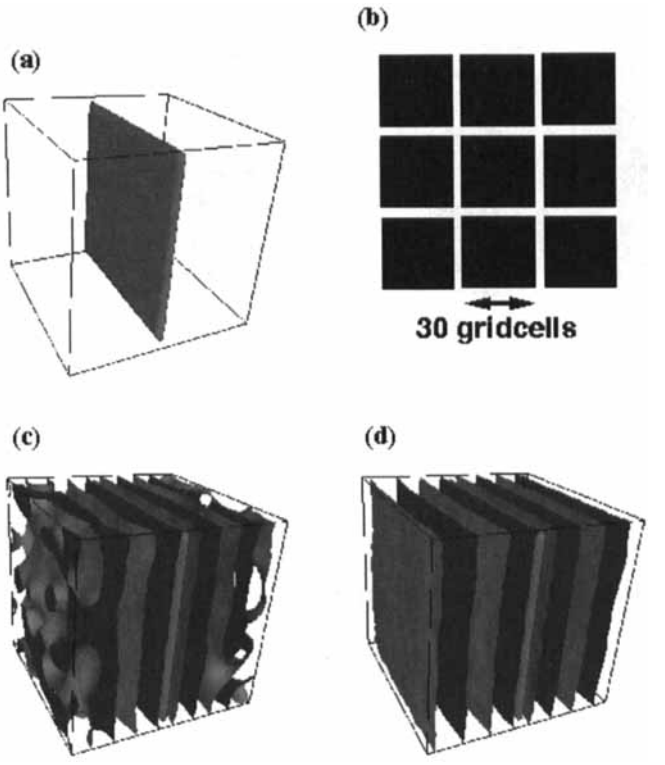

FIGURE 4(a–d) Lamellar formation of an A_8B_8 copolymer melt in the presence of square plates of one grid-cell thickness. The interaction of polymer blocks with the surface is $\beta\varepsilon_{AM}\nu^{-1} = -1.0$ and $\beta\varepsilon_{BM}\nu^{-1} = 1.0$: (a) View of filler particle in simulation box, (b) Space filled with filler particles (the slots between filler particles are drawn as white lines), (c) Morphology of A beads (isolevel $\nu\rho_A = 0.5$) in one simulation box at $\tau = 500$, (d) Same for $\tau = 2000$.

Downloaded At: 18:55 14 January 2011

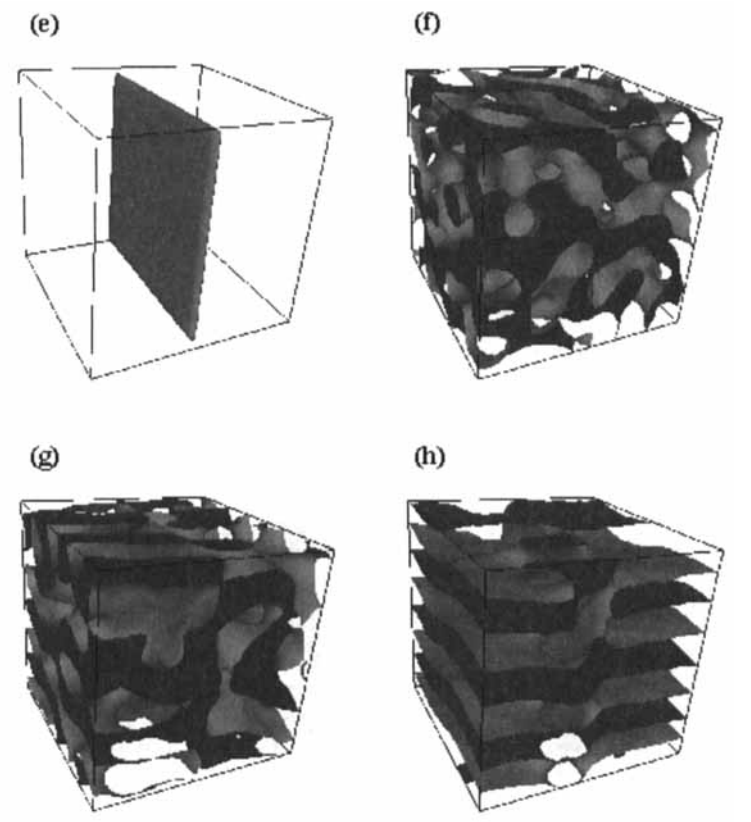

FIGURE 5(e–h) Lamellar formation of an A_8B_8 copolymer melt in the presence of the same filler particle as previous figure. Moreover, there is no interaction between the polymer beads and boundaries of the filler particles: (e) View of filler particle in simulation box, (f) Morphology of A beads (isolevel $\nu\rho_A = 0.5$) in one simulation box at $\tau = 500$, (g) Same for $\tau = 4000$, (h) Final morphology at $\tau = 10000$.

DISCUSSION AND CONCLUSION

In this paper we described the theoretical basis and some application of a new model for computer simulation of time evolution of mesoscale structures of complex polymer liquids. We describe some other possible applications of the proposed method. The investigation of these applications is in progress.

One of the main questions in industrial emulsion polymerizations is to produce a latex or polymer with any desired morphology, composition, sequence distribution, molecular weight distribution *etc.* A specific example

Downloaded At: 18:55 14 January 2011

is given by the core-shell techniques in which one type of (co)polymer is grown around a core of another type. In paints the core polymer may provide gloss and mechanical stability whereas the shell might contain a rubbery polymer to provide a uniform surface coating. The final morphology that is obtained in the production process determines the quality of the product to a very large extent and hence prediction of the morphology based on production process parameters is desirable. The morphology is controlled by both thermodynamic (the micro-phase separation process) and kinetic (the reaction process) principles. Several practical applications are within direct reach. An example of a one-stage core-shell technique that has been described in literature concerns the mixing of silicone oils (containing Si—H and vinyl groups) and vinyl monomers emulsified in water. After a (cross-linking) reaction of Si—H and Si—CH=CH2 (kinetics) the hydrophilic monomers are excluded to the surface layer (thermodynamics) and a core-shell morphology results.

Another potential application is the investigation of the stability of polymer surfactant protected emulsions. In particular, many industrial systems contain a specified mixture of different surfactants, so as to provide a certain stability of the interphase. Thus the application of the emulsions is controlled by the nature of the surfactant mixture. Within the described method it is relatively easy to study the synergetic effects of surfactant composition and architecture, and the way processing conditions influence the emulsion stability and morphology.

Downloaded At: 18:55 14 January 2011

References

[1] Qiwei He, D. and Nauman, E. B. (1997). *Chemical Engineering Science*, **52**(4), 481–496.
[2] Gonnella, G., Orlandini, E. and Yeomans, J. M. (1997). *Physical Review Letters*, **78**(9), 1695–1698.
[3] Pätzold, G. and Dawson, K. (1996). *J. Chem. Phys.*, **104**(15), 5932–5941.
[4] Kodama, H. and Komura, S. (1997). *J. Phys. II France*, **7**(1), 7–14.
[5] Ohta, T., Nozaki, H. and Doi, M. (1990). *Physics Letters A*, **145**(6,7), 304–308.
[6] Cahn, J. W. and Hilliard, J. E. (1958). *J. Chem. Phys.*, **28**, 258–267.
[7] Oono, Y. and Puri, S. (1987). *Phys. Rev. Let.*, **58**, 836–839.
[8] de Gennes, P. G. (1980). *J. Chem. Phys.*, **72**, 4756–4763.
[9] Maurits, N. M. and Fraaije, J. G. E. M. (1997). *J. Chem. Phys.*, **106**, 6730–6743.
[10] Fraaije, J. G. E. M. (1993). *J. Chem. Phys.*, **99**, 9202–9212.
[11] Fraaije, J. G. E. M., van Vlimmeren, B. A. C., Maurits, N. M., Postma, M., Evers, O. A., Hoffmann, C., Altevogt, P. and Goldbeck-Wood, G. (1997). *J. Chem. Phys.*, **106**(10), 4260–4269.
[12] Maurits, N. M., van Vlimmeren, B. A. C. and Fraaije, J. G. E. M. (1997). *Phys. Rev. E*, **56**(1), 816–825.
[13] Maurits, N. M. and Fraaije, J. G. E. M. (1997). *J. Chem. Phys.*, **107**, 5879–5889.
[14] van Vlimmeren, B. A. C. and Fraaije, J. G. E. M. (1996). *Comp. Phys. Comm.*, **99**, 21–28.
[15] Maurits, N. M., Altevogt, P., Evers, O. A. and Fraaije, J. G. E. M. (1996). *Comp. Pol. Sci.*, **6**(1,2), 1–8.

[16] Kawakatsu, T. (1997). *Phys. Rev. E*, **56**(3), 3240–3250.
[17] Hasegawa, R. and Doi, M. (1997). *Macromolecules*, **30**(10), 3086–3089.
[18] van Vlimmeren, B. A. C., Maurits, N. M., Zvelindovsky, A. V., Sevink, G. J. A. and Fraaije, J. G. E. M. (1999). *Macromolecules*, **32**(10), 646–656.
[19] Zvelindovsky, A. V., Sevink, G. J. A., van Vlimmeren, B. A. C., Maurits, N. M. and Fraaije, J. G. E. M. (1998). *Phys. Rev. E*, **57**(5), R4879–R4882.
[20] Alexandridis, P., Olsson, U. and Lindmann, B. (1995). *Macromolecules*, **28**(23), 7700–7710.
[21] Kodama, H. and Doi, M. (1996). *Macromolecules*, **29**(7), 2652–2658.
[22] Fredrickson, G. H. (1994). *J. Rheol.*, **38**(4), 1045–1067.
[23] Bird, R. B., Hassager, O. and Armstrong, R. C. (1987). *Dynamics of polymeric liquids*, Wiley, New York.
[24] Schmittmann, B. and Zia, R. K. P. (1994). Statistical mechanics of driven diffusive systems. In: Domb, C. and Lebowitz, J., Eds., *Phase Transitions and Critical Phenomena*, Academic, London.
[25] Grosberg, A. Y. and Khokhlov, A. R. (1994). *Statistical Physics of Macromolecules*, AIP Press, New York.
[26] Doi, M. and Chen, D. (1989). *J. Chem. Phys.*, **90**(10), 5271–5279.
[27] Ohta, T., Enomoto, Y., Harden, J. L. and Doi, M. (1993). *Macromolecules*, **26**, 4928–4934.
[28] Chen, Z. R., Kornfield, J. A., Smith, S. D., Grothaus, J. T. and Satkowski, M. M. (1997). *Science*, **277**, 1248–1253.

Downloaded At: 18:55 14 January 2011